The novel synthesized 2-(3-(methylamino)phenyl)-6-(pyrrolidin-1-yl)quinolin-4-one (Smh-3) compound induces G_2/M phase arrest and mitochondrial-dependent apoptotic cell death through inhibition of CDK1 and AKT activity in HL-60 human leukemia cells

SHIH-MING HUANG[1], JAI-SING YANG[2], SHIH-CHANG TSAI[3], MING-HUA CHEN[1], MEI-HUA HSU[1], HUI-YI LIN[1], LI-CHEN CHOU[1], JO-HUA CHINAG[5], KUO-HSIUNG LEE[6], LI-JIAU HUANG[1] and SHENG-CHU KUO[1,4]

[1]Graduate Institute of Pharmaceutical Chemistry, Departments of [2]Pharmacology and [3]Biological Science and Technology, [4]Chinese Medicine Research and Development Center, China Medical University, Taichung 404; [5]Department of Life Sciences, National Chung Hsing University, Taichung 402, Taiwan, R.O.C.; [6]Natural Products Research Laboratories, UNC Eshelman School of Pharmacy, University of North Carolina, Chapel Hill, NC 27599-7568, USA

Received December 2, 2010; Accepted January 28, 2011

DOI: 10.3892/ijo.2011.952

Abstract. 2-Phenyl-4-quinolone series compounds have exhibited growth inhibitory influence on several human cancer cell lines. In this study, we investigated the effects of 2-(3-(methylamino)phenyl)-6-(pyrrolidin-1-yl)quinolin-4-one (Smh-3) on viability, cell cycle and apoptotic cell death which occurred in different leukemia cell lines (HL-60, U937 and K562) in a dose- and time-dependent manner, but which did not obviously impair the viability of normal human umbilical vein endothelial cells (HUVEC) *in vitro*. The approximate IC_{50} was 103.26±4.59 nM for a 48 h treatment in HL-60 cells. Cell cycle analysis showed that 100 nM Smh-3 induced significant G_2/M arrest in examined cells. Within 0, 12, 24 and 48 h of treatment, Smh-3 inhibited CDK1 activity and decreased protein levels of CDK1, cyclin A and cyclin B. Smh-3-induced chromatin condensation and DNA fragmentation were determined by DAPI and TUNEL staining. Cell apoptosis was significantly reduced after pretreatment with a pan-caspase inhibitor (Z-VAD-fmk) and results indicated that Smh-3-induced apoptosis was mainly mediated by activation of the caspase cascade in HL-60 cells. Results from colorimetric assays and Western blot analysis indicated that activities of caspase-9, -7 and -3 were promoted in Smh-3-treated HL-60 cells during cell apoptosis. Smh-3-induced apoptosis in HL-60 cells was accompanied by an apparent increase in ROS production, and protein levels of cytosolic cytochrome *c*, apoptotic protease activating factor-1 (Apaf-1) and apoptosis-inducing factor (AIF). Strikingly, Smh-3 induced apoptosis in HL-60 cells by simultaneously suppressing protein levels of AKT, p-AKT, p-mTOR and p-BAD and inducing BAD protein levels. Taken together, we conclude that Smh-3 acts against leukemia cells *in vitro* via G_2/M phase arrest, down-regulation of AKT activity and induction of mitochondrial-dependent apoptotic pathways.

Correspondence to: Dr Sheng-Chu Kuo or Dr Li-Jiau Huang, Graduate Institute of Pharmaceutical Chemistry, China Medical University, No. 91, Hsueh-Shih Road, Taichung 404, Taiwan, R.O.C.
E-mail: sckuo@mail.cmu.edu.tw
E-mail: ljhuang@mail.cmu.edu.tw

Key words: Smh-3, G_2/M arrest, apoptosis, CDK1, AKT, human leukemia HL-60 cells

Introduction

Leukemia is one of the hematologic malignancies in human population. About 4.0 per 100,000 people die of leukemia each year in Taiwan based on the report of the Department of Health, R.O.C. (Taiwan) in the 2009 report (http://www.doh.gov.tw/EN2006/index_EN.aspx). Leukemia involves progressive disruption of cell differentiation, proliferation and apoptosis (1). Bone marrow transplant, radiotherapy and chemotherapy are applied for the treatment of leukemia patients (2).

The novel synthesized compounds, designed for providing chemotherapeutic effectiveness, are not detrimental to normal cells, which exert specific cytotoxic effects on leukemia cells through cell cycle arrest and apoptosis (3). Cyclin-dependent protein kinases (CDKs) and cyclins play important regulatory roles in cell cycle transition (4). Particularly, G_2-M transition is regulated by cyclin-dependent protein kinase 1 ($p34^{cdc2}$; CDK1) and cyclins A, B (5). Apoptosis is characterized by a series of morphological changes involving cell shrinkage and chromatin condensation (6). At least, two distinct pathways are involved in apoptotic cell death. The intrinsic pathway involves disrupting the mitochondrial membrane and releasing

cytochrome *c*, Apaf-1, AIF and pro-caspase-9 into the cytosol. The extrinsic pathway of apoptosis requires death receptors and ligand interaction such as FasL/Fas, TNF/TNFR and then to activate downstream caspase-8 (7-9). Both intrinsic and extrinsic pathways induce the activation of caspase-7 and -3 (10). A recent study has also demonstrated that the BCL-2 family proteins such as BAD can regulated mitochondria-mediated apoptotic pathway (11). It is thought that the ability of BAD to bind to BCL-2 is abrogated when BAD becomes phosphorylated at Ser136 by AKT protein kinase (12,13).

In the present study, we have designed and synthesized a series of 2-phenyl-4-quinolone compounds as novel anti-leukemia agents. 2-(3-(methylamino)phenyl)-6-(pyrrolidin-1-yl)quinolin-4-one (Smh-3), as shown in Fig. 1, is a most potential candidate for anti-leukemia activities. However, neither the cytotoxic effects of Smh-3 on leukemia cells and normal cells, nor the molecular mechanisms underlying its anticancer activity have been investigated. Therefore, this study investigated the molecular mechanisms of Smh-3 in anti-leukemia effects on HL-60 cells *in vitro*.

Materials and methods

Chemicals and reagents. Smh-3 (2-(3-(methylamino)phenyl)-6-(pyrrolidin-1-yl) quinolin-4-one; Fig. 1) was synthesized in our laboratory, Graduate Institute of Pharmaceutical Chemistry, College of Pharmacy, China Medical University. Propidium iodide (PI), RNase A, Triton X-100 and proteinase K were purchased from Sigma Chemical Co. (St. Louis, MO). The Z-VAD-fmk (a pan-caspase inhibitor) was purchased from R&D Systems (Minneapolis, MN, USA). Sources of antibodies used in this study were as follows: polyclonal antibodies specific for phospho-GSK-3 α/β (Ser219), phospho-AKT (Ser473), phospho-mTOR (Ser 2481), phospho-BAD (Ser136), caspase-8, -9, -7 and -3 were obtained from Cell Signaling Technology Inc. (Danvers, MA, USA) and monoclonal antibodies specific for cyclin B, CDK1, cyclin A, cytochrome c, Apaf-1, AKT, mTOR, BAD and actin and all peroxidase-conjugated secondary antibodies were obtained from Santa Cruz Biotechnology, Inc. (Santa Cruz, CA, USA). Monoclonal antibodies specific for AIF was purchased from Abcam Inc. (Cambridge, MA, USA). Enhanced chemiluminescence (ECL) was purchased from Pierce Chemical (Rockford, IL, USA).

Cell culture. The leukemia cell lines HL-60 (human promyelocytic leukemia), U937 (human lymphoma cancer cell), K562 (human chronic myelogenous leukemia), and HUVEC (human umbilical vein endothelial cells) were purchased from Culture Collection and Research Center (CCRC), Food Industry Research and Development Institute (Hsinchu, Taiwan). Cells were cultured in RPMI-1640 medium (Invitrogen, Carlsbad, CA, USA) and supplemented with 10% heat-inactivated fetal calf serum (FCS) (HyClone, Logan, UT, USA), 100 U/ml penicillin, 100 μg/ml streptomycin and 2 mM L-glutamine at 37˚C in a 5% CO_2 humidified incubator. The HUVEC were passaged at preconfluent densities using a solution containing 0.05% trypsin and 0.5 mM EDTA (Invitrogen) (13).

Determinations of cell viability. Cells ($2.5x10^5$/well) were seeded in each well of 24-well plates and incubated with 0, 50, 100, 200 and 400 nM Smh-3 for 0, 24 and 48 h. Cells were harvested, washed and re-suspended with phosphate-buffered saline (PBS) containing 4 μg/ml PI, and then analyzed by using a PI exclusion method and flow cytometry (FACSCalibur™, Becton-Dickinson, NJ, USA) equipped with a laser at 488 nm wavelength. The percentage of cell viability was calculated as a ratio of the number of Smh-3-treated cells to that of 0.1% DMSO as a vehicle-control group (14,15). Viability assays were performed in triplicate from three independent experiments. The 50% inhibitory concentration (IC_{50}) of Smh-3 was calculated using the software of dose-effect analysis with microcomputers as described previously (13).

Cell morphology. HL-60 cells ($2x10^5$ cells/well) were maintained in 24-well plates with RPMI-1640 medium and then were treated with 0, 50, 100 and 200 nM of Smh-3. Cell morphology was examined and photographed under a phase contrast microscope. Chromatin condensation was detected using the DAPI (4,6-diamidino-2-phenylindole dihydrochloride) staining method. HL-60 cells were treated with 100 nM Smh-3 for 0, 12, 24 and 48 h. After incubation for the indicated time, HL-60 cells were fixed gently by putting 70% ethanol, stained with DAPI, and then photographed using a fluorescence microscope as described previously (14,16).

DNA content and cell cycle distribution analysis. HL-60 cells were seeded in 24-well cell culture plates at a density of $2.5x10^5$ cells/well, and incubated with 100 nM Smh-3 for 0, 12, 24 and 48 h. For determination of cell cycle phase and apoptosis, cells were fixed gently by putting 70% ethanol in -20˚C overnight, and then re-suspended in PBS containing 40 μg/ml PI, 0.1 mg/ml RNase and 0.1% Triton X-100 in dark room for 30 min. Cell cycle distribution and apoptotic nuclei were determined by flow cytometry as described previously (13,17).

CDK1 kinase assay. CDK1 kinase activity was analyzed according to the protocol of Medical & Biological Laboratories CDK1 kinase assay kit (MBL International, Nagoya, Japan). In brief, the ability of cell extract prepared from each treatment was measured to phosphorylate its specific substrate, MV peptide as described previously (13,18).

TUNEL assay. HL-60 cells were seeded in 24-well cell culture plates at a density of $2.5x10^5$ cells/well, and then incubated with 100 nM Smh-3 for 0, 24, 48 and 72 h. For the specific inhibitor assay, cells were seeded in 24-well plates, and then pretreated with a pan-caspase inhibitor (Z-VAD-fmk) for 1 h, followed by treatment with or without 100 nM Smh-3. After incubation for the indicated time, *in situ* apoptosis detection of DNA fragmentation was determined by using a terminal deoxyribonucleotide transferase-mediated dUTP nick-end labeling (TUNEL) assay (Roche Diagnostics, Hillsdale, MI, USA). Following TUNEL staining, all samples were washed once and re-suspended in 0.5 ml of PBS containing PI (10 μg/ml) and DNase free-RNase A (200 μg/ml). TUNEL positive cells were analyzed by flow cytometry. The median fluorescence intensity was quantified by BD Pro CellQuest software. TUNEL assays were performed in triplicate from three independent experiments as described previously (13).

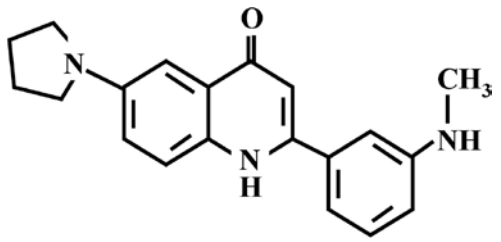

Figure 1. Chemistry structure of Smh-3 (2-(3-(methylamino)phenyl) -6-(pyrrolidin-1-yl) quinolin-4-one).

Caspase activity assay. HL-60 cells ($2.5x10^6$ cells/well) were seeded in 6-well cell culture plates and incubated with 100 nM Smh-3 for 48 h. Cells were lysed in lysis buffer (50 mM Tris-HCl (pH 7.4), 1 mM EDTA, 10 mM EGTA, 10 mM digitonin and 2 mM DTT). About 50 μg of cytosol proteins were incubated with caspase-9, -8, -7 and -3 specific substrates (R&D System) for 1 h at 37˚C. The caspase activity was determined by measuring OD 405 as described previously (19).

Western blotting. HL-60 cells were seeded in 10 cm-dishes at an initial concentration of $1x10^7$ cells and incubated with 100 nM Smh-3 for 0, 12, 24 and 48 h. Cytosolic fraction and total protein were prepared and determined. Equal amounts of protein (30 μg) were separated by 10-12% sodium dodecyl sulfate polyacrylamide gel electrophoresis (SDS–PAGE) and electro-transferred to a nitrocellulose membrane by using iBot™ Dry Blotting System (Invitrogen). Blots were blocked in PBST buffer (0.05% Triton X-100 in PBS) containing 5% non-fat milk for 1 h, and incubated with specific primary antibodies at 4˚C overnight. The membrane was washed with PBST buffer and incubated with secondary antibodies conjugated horseradish peroxidase (HRP). The specific protein was detected by using enhanced chemiluminescence kits (Amersham, ECL Kits) as described previously (13,19).

Determination of reactive oxygen species (ROS). Approximately $2x10^5$ cells/well of HL-60 cells in 24-well plates were treated with 100 nM Smh-3 and incubated for 0, 3, 6, 12 and 24 h. At the end of incubation, cells from each treatment were harvested by centrifugation, washed twice by PBS, and then re-suspended in 2,7-dichlorodihydrofluorescein diacetate (DCFH-DA; 10 μM) for ROS determination. Cells were incubated for 30 min at 37˚C in the dark room and analyzed immediately by flow cytometry as described previously (15,19).

In vitro cell AKT kinase assay. This assay was performed followed as the protocol of the manufacturer's instructions from an AKT kinase assay Kit (Cell Signaling Technology, Beverly, MA, USA). In brief, about $1x10^6$ cells/well of HL-60 cells in a 75-T flask were treated with 0, 50, 100, 200 and 400 nM of Smh-3 for 2 h. Cells were then harvested, washed twice with PBS, and lyzed in ice-cold lysis buffer provided in this kit. The 200 mg of protein from each time-point treatment were immunoprecipitated with 2 mg of anti-AKT antibody overnight. All samples were extensively washed, and then the immunoprecipitates were incubated with 1 mg of glycogen synthase kinase-3 α/β (GSK-3 α/β) fusion protein substrate in 50 μl of kinase buffer for 30 min at 30˚C. Reactions were stopped with SDS loading buffer. The samples were separated on 12% SDS-PAGE, and the phospho-GSK-3 α/β (Ser219) was detected by immunoblotting (20).

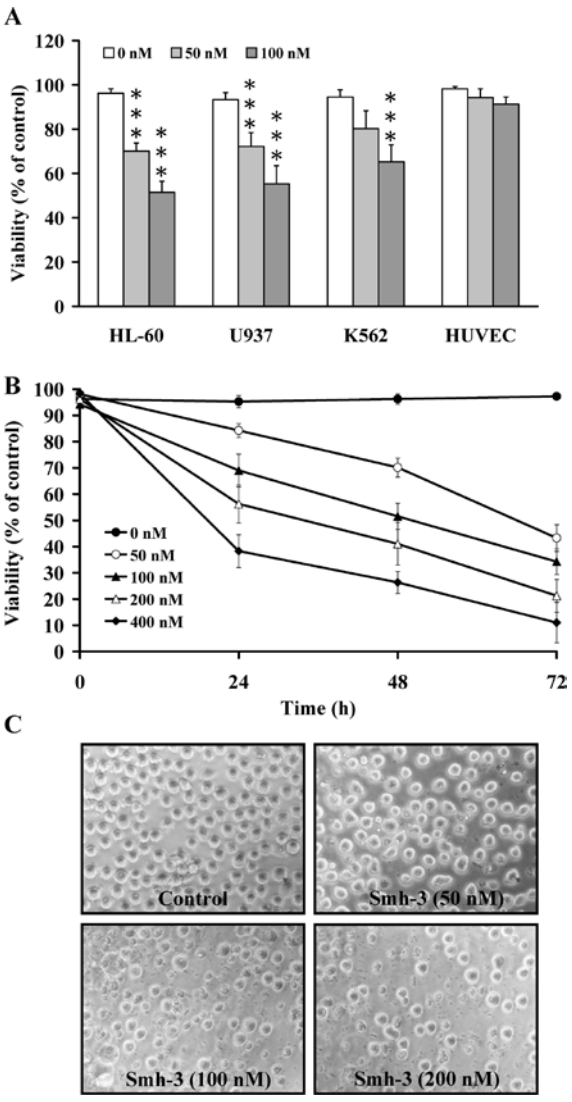

Figure 2. Effects of Smh-3 on cell viability and morphological changes in human leukemia cell lines. Human leukemia cells (HL-60, U937 and K562) and HUVEC were treated with 0, 50, 100 nM of Smh-3 for 48 h and then cell viability was determined by a PI exclusion method and flow cytometry (A). HL-60 cells were exposed to 0, 50, 100, 200 and 400 nM of Smh-3 for 0, 24, 48 and 72 h, and cell viability was determined and measured (B). The data shown are mean ± SEM of three independent experiments. ***P<0.001 vs. 0 nM treatment. Cells were treated with 0, 50, 100 and 200 nM of Smh-3 for 48 h, and photographed under a phase-contrast microscope at a magnification x200 (C).

Statistical analysis. Data are presented as the mean ± SEM for the indicated number of separate experiment. Statistical analyses of data were performed by Student's t-test, and *P<0.05, ***P<0.001 were considered significant.

Results

Smh-3 inhibited cell growth of human leukemia cells. Initially, cells were determined the growth inhibition effects of Smh-3 on cell viability by using a PI exclusion assay and flow cytometric analysis. As shown in Fig. 2A, Smh-3 inhibited cell growth of

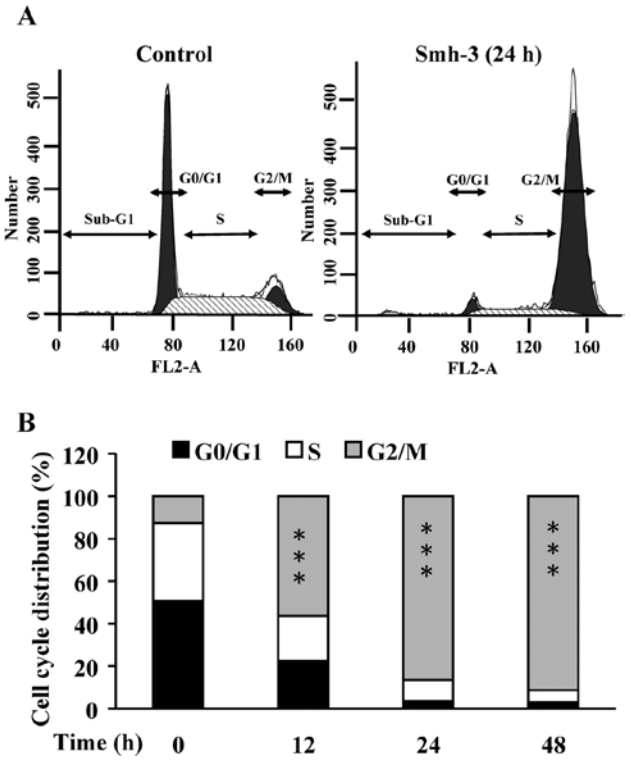

Figure 3. Smh-3 promotes G_2/M phase arrest in HL-60 cells. Cells were treated with 100 nM Smh-3 for 0, 12, 24 and 48 h, and then harvested for cell cycle distribution by flow cytometry (A). Bar graph representation of the percentage in different phases of the cell cycle distribution (B).

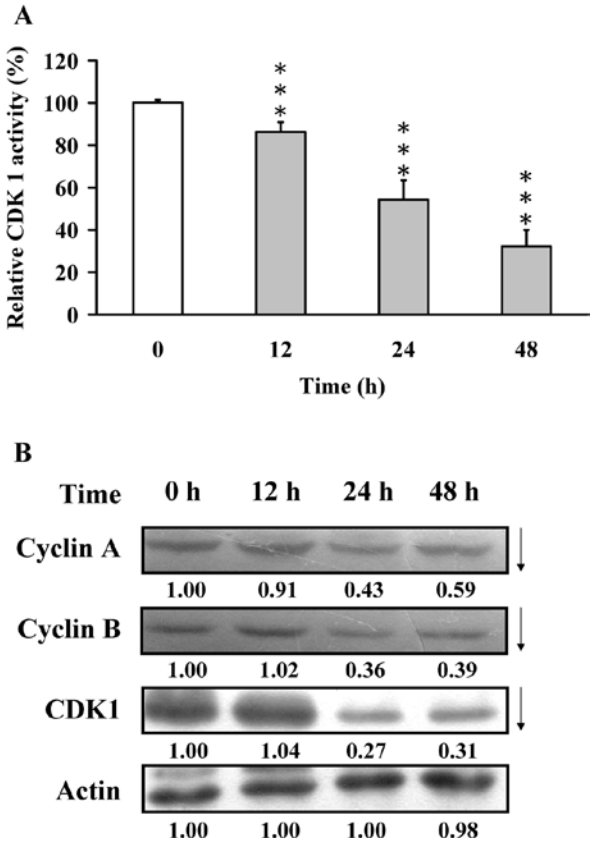

Figure 4. Smh-3 inhibits CDK1 activity and affects G_2/M phase-associated protein levels in HL-60 cells. Cells were treated with 100 nM Smh-3 for 0, 12, 24 and 48 h, and then harvested for examining the CDK1 activity (A). Cells were incubated with 100 nM Smh-3 for 0, 12, 24 and 48 h and then harvested, total protein was lysed for the detection of the protein levels of cyclins A, B and CDK1 by Western blot analysis (B).

HL-60, U937 and K562 cells in a dose-dependent manner. Smh-3 shows much less cytotoxic effect on the normal HUVE than that on HL-60 cells as compared this effect of Smh-3 on HL-60 to normal HUVEC cells (Fig. 2A). Smh-3 inhibited cell growth of HL-60 cells in a dose- and time-dependent manner (Fig. 2B). The half maximal inhibitory concentration IC_{50} for 48 h treatment of Smh-3 in HL-60 cells was 103.26±4.59 nM. It can be seen in Fig. 2C and indicated that Smh-3 induced cell morphological changes, and decreased the cells number in HL-60 cells. Apoptotic HL-60 cells showed smaller, round and blunt in size after Smh-3 exposure, and these effects are dose-dependent (Fig. 2C).

Smh-3 induced G_2/M phase arrest by decrease CDK1 activity in HL-60 cells. We investigated the possible mechanisms and whether Smh-3 is able to promote cell cycle arrest in HL-60 cells. As shown in Fig. 3, 100 nM Smh-3 induced cell cycle arrest in G_2/M phase in HL-60 cells and this effect was time-dependent. We also examined the CDK1 activity in Smh-3-treated HL-60 cells. Results shown in Fig. 4A indicate that Smh-3 caused a significant decrease in CDK1 activity for 12, 24, and 48 h treatment. We characterized the cell cycle-regulated protein levels in G_2/M phase. As shown in Fig. 4B, Smh-3 caused a decrease the protein levels of cyclins A, B and CDK1 in HL-60 cells. Our results suggest that cyclins A, B and CDK1 activities play important roles in G_2/M phase arrest in Smh-3-treated HL-60 cells.

Smh-3 induced chromatin condensation and DNA fragmentation in HL-60 cells. To investigate the incidence of chromatin condensation in Smh-3-treated HL-60 cells, we assessed the nuclear chromatin changes by DAPI staining. As shown in Fig. 5A, cells exhibited nuclear shrinkage and chromatin condensation after incubation with 100 nM Smh-3 for 12, 24 and 48 h. We also demonstrated that Smh-3 induced DNA fragmentation which was examined by TUNEL staining and flow cytometric analysis as shown in Fig. 5B. Smh-3 induced DNA fragmentation (TUNEL positive cells) in HL-60 cells and this response was increased in a time-dependent manner. Based on our results, it is suggested that Smh-3 induced chromatin condensation and DNA fragmentation for cell apoptosis in HL-60 cells *in vitro*.

Smh-3 stimulates the activities of caspase-3, -7 and -9 in HL-60 cells. To verify if caspase activity is involved in Smh-3-induced apoptosis in HL-60 cells, the cells were pretreated with 10 μM Z-VAD-fmk (a pan-caspases inhibitor) and exposed to 100 nM Smh-3. The cells were harvested for measuring the TUNEL positive cells by flow cytometric assay. The results are shown in Fig. 6A and revealed that Z-VAD-fmk decreased the percentage of TUNEL positive cells in Smh-3-treated HL-60 cells. Our finding indicated that Smh-3-induced apoptosis was through an increase of caspase activity. To examine whether Smh-3-induced apoptosis is involved in the activations of caspase cascades, cells were harvested after exposure to 100 nM Smh-3 and then the

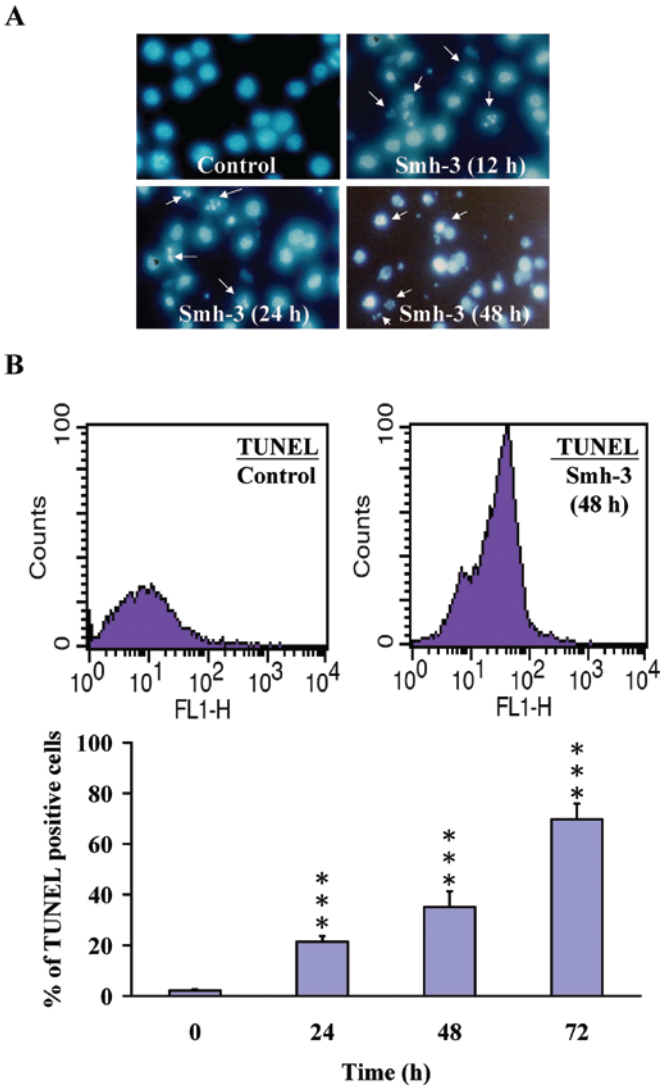

Figure 5. Smh-3 induced chromatin condensation and DNA fragmentation in HL-60 cells. For detecting chromatin condensation, cells were treated with 100 nM Smh-3 for 0, 12, 24 and 48 h, and were stained by DAPI staining as described in Materials and methods (A). The DNA fragmentation was determined by TUNEL assay and analyzed by flow cytometry (B). The data shown are the mean ± SEM of three independent experiments. ***P<0.001 vs. 0 h treatment.

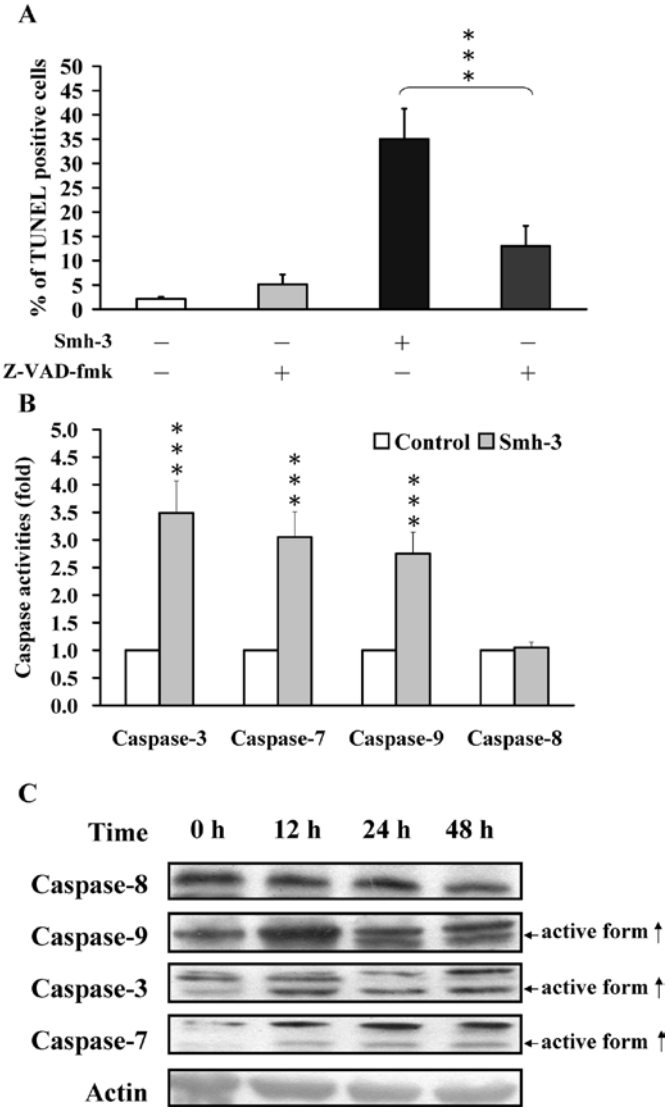

Figure 6. Smh-3 increased the caspase-3, -7 and -9 activities and protein levels in HL-60 cells. Cells were pretreated with or without 10 μM pan-caspase inhibitor (Z-VAD-fmk) and then were treated with 100 μM Smh-3 for 48 h. The apoptotic cells were determined by TUNEL assay and analyzed by flow cytometry (A). Cells were treated with 100 nM Smh-3 for 48 h and the whole-cell lysate was subjected to caspase-3, -7, -9 and -8 activity assay (B). The data shown are mean ± SEM of three independent experiments. ***P<0.001 vs. control. Cells were treated with 100 nM Smh-3 for 0, 12, 24 and 48 h, and then harvested total protein lysed for the detection the protein levels of caspase-8, -9, -3 and -7 by Western blot analysis (C).

activities of caspase-3, -7, -8 and -9 were determined by colorimetric assays or examined the protein levels of caspase-3, -7, -8 and -9 by Western blotting. As shown in Fig. 6B, Smh-3 promoted the activation of caspase-3, -7 and -9, but not caspase-8 after 48 h treatment. Therefore, Smh-3 increased the active form levels of caspase-3, -7 and -9 in a time-dependent manner (Fig. 6C). Our results suggest that Smh-3-triggered apoptosis may be mediated through mitochondria-dependent signaling pathway in HL-60 cells.

Smh-3 induced production of reactive oxygen species (ROS) and release of the apoptosis-associated proteins in HL-60 cells. To verify if ROS are involved in Smh-3-induced apoptosis in HL-60 cells, the cells were exposed to 100 nM Smh-3 for 0, 3, 6, 12 and 24 h, and then harvested for measurement in the level of ROS production by flow cytometric assay. The results in Fig. 7A indicated that Smh-3 promoted the ROS production from 3 to 24 h time-dependently. Smh-3 (100 nM) increased the protein levels of cytosolic cytochrome *c*, AIF and Apaf-1 (Fig. 7B). Our results indicated that Smh-3-induced cell death may be mediated through the mitochondria-dependent apoptotic signaling pathways in HL-60 cells.

Smh-3 inhibited the activity of AKT and down-regulated the expression of phospho-BAD in HL-60 cells. To examine the involvement of AKT pathway in Smh-3-regulated apoptosis in HL-60 cells, we assessed the effects of Smh-3 on AKT activity at 0, 50, 100, 200 and 400 nM of Smh-3 for 2 h treatment. The protein levels of phospho-AKT and phospho-mTOR after treatment with 100 nM of Smh-3 for 0, 1, 2 and 4 h were investigated. Our results in Fig. 8A show that Smh-3

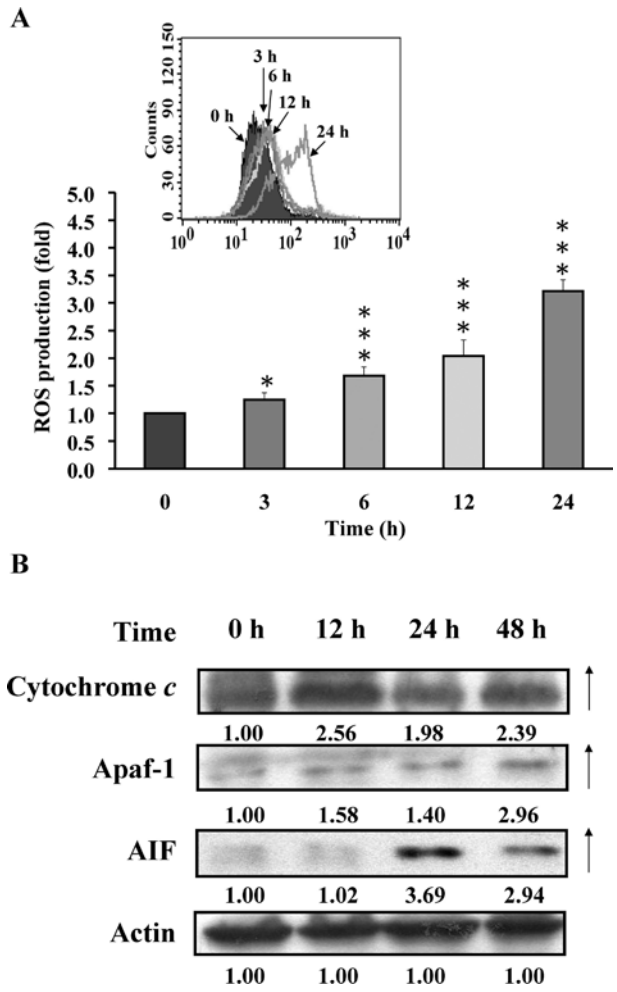

Figure 7. Smh-3 enhances the ROS production and affects the apoptosis-associated protein levels of mitochondria-dependent pathway in HL-60 cells. Cells were treated with 100 nM Smh-3 for 0, 3, 6, 12 and 24 h. The level of ROS production was stained with 2,7-dichlorodihydrofluorescein diacetate (DCFH-DA). The stained cells were determined by flow cytometry as described in Materials and methods (A). Cells were treated with 100 nM Smh-3 for 0, 12, 24 and 48 h and then harvested cytosolic lysate for the detection the protein levels of cytochrome *c*, Apaf-1 and AIF by Western blot analysis (B). The data shown are mean ± SEM of three independent experiments. ***P<0.001 vs. 0 h treatment.

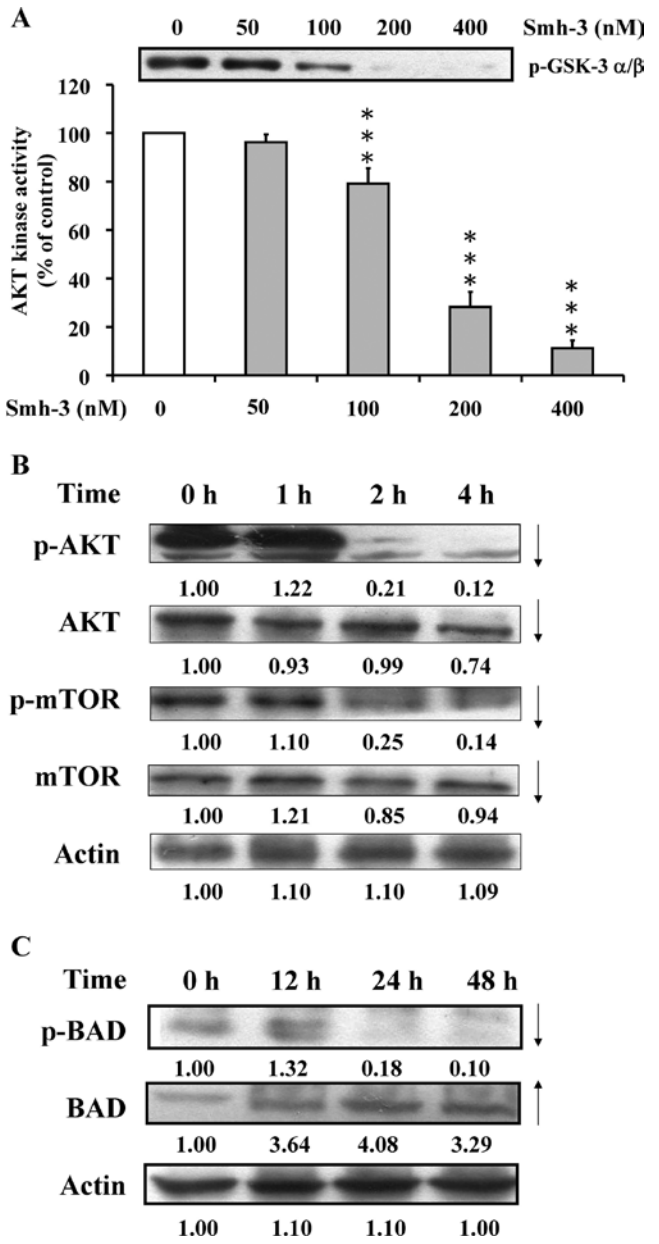

Figure 8. Smh-3 inhibits the AKT activity and affects the BAD protein level in HL-60 cells. Cells were treated with 0, 50, 100, 200 and 400 nM of Smh-3 for 2 h and then were harvested for examining the AKT activity as described in Materials and methods (A). Cells were treated with 100 nM of Smh-3 for 0, 1, 2 and 4 h, and then harvested total protein lysed for the detection the protein levels of AKT, p-AKT, mTOR, p-mTOR (B) and p-BAD, BAD (C) by Western blot analysis. The data shown are mean ± SEM of three independent experiments. ***P<0.001 vs. 0 h or 0 nM treatment.

decreased the AKT activity after treatment with 50 to 400 nM of Smh-3 and this effect is dose-dependent. In Fig. 8B, results from Western blot analysis show that Smh-3 caused a decrease in protein levels of phospho-AKT, AKT, phospho-mTOR and mTOR in HL-60 cells. It is reported that BAD is a major regulator of AKT signaling (10), we next determined the effect of Smh-3 on the protein levels of BAD and phospho-BAD in HL-60 cells. As seen in Fig. 8C, we found an increase in the expression of BAD, but a decrease in the expression of phospho-BAD in a time-dependent manner. Our data suggest that Smh-3-affected apoptotic cell death in HL-60 cells is through inhibition of the AKT activity, leading to the decrease in the level of phospho-BAD protein.

Discussion

Several reports have been demonstrated that 2-phenyl-4-quinolones series compounds exhibited growth inhibitory effects on several human cancer cell lines (18,21). 2-phenyl-4-quinolone series compounds might inhibit CDK1 activity and act as anti-mitotic agents (18). In recent years, we have designed and synthesized a new series of 2-phenyl 6-pyrrolidinyl-4-quinazolinone derivatives as new anti-leukemia agents and Smh-3 (Fig. 1) (2-(3-(methylamino)phenyl)-6-(pyrrolidin-1-yl) quinolin-4-one) is the most potential compound against cancer cells *in vitro*. However, the growth inhibition effects of Smh-3 on leukemia cells and normal cells or the molecular mechanisms underlying its anti-leukemia activity have not been clarified. In this study, we first demonstrated that Smh-3 induced growth

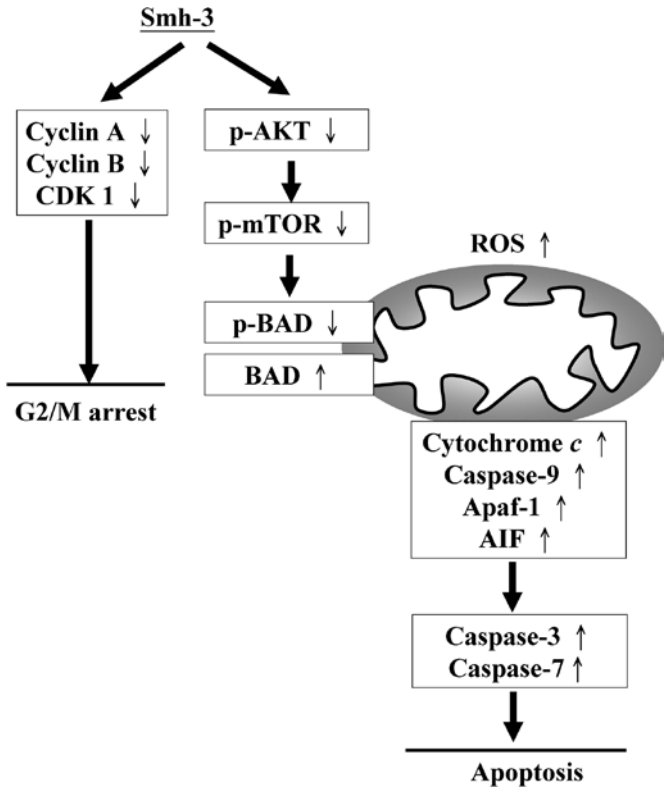

Figure 9. The proposed model shows that the Smh-3 induces G_2/M phase arrest and apoptotic cell death in human leukemia HL-60 cells.

inhibitory effects through G_2/M phase arrest (Fig. 3) and induction of apoptosis (Fig. 5) in HL-60 cells. Moreover, Smh-3 has much less cytotoxic effect on HUVEC than that on HL-60 cells (Fig. 2A). It is important for Smh-3 to be used in leukemia patients with decreasing side-effects.

We selected the closest concentration to IC_{50} (100 nM) of Smh-3 for determining anti-leukemia activity. Results are summarized as follows: i) HL-60 cells were treated with Smh-3 for 12-48 h, causing G_2/M arrest (Fig. 3). ii) Smh-3 decreased CDK1 activity as well as protein levels of cyclins A, B and CDK1 in HL-60 cells (Fig. 4). iii) Smh-3 caused activation of caspase-9, -7 and -3 in HL-60 cells (Fig. 6). iv) Smh-3 caused a decrease in AKT activity and protein levels after 2 h treatment in HL-60 cells (Fig. 8). v) Smh-3 down-regulated the protein level of p-BAD and up-regulated protein levels of cytosolic cytochrome *c*, AIF and Apaf-1 in HL-60 cells (Figs. 7 and 8). Taken together, we suggest that Smh-3 induced apoptotic cell death through the mitochondria-dependent apoptotic pathway by inhibiting AKT activity in HL-60 cells.

Our results showed that Smh-3 promoted the ROS production in HL-60 cells and this effect is time-dependent (Fig. 7A). HL-60 cells were pretreated with ROS scavenger, 10 mM NAC, which led to increase in the viable HL-60 cells when compared to the only Smh-3-treated cells (data not shown). The results suggest that ROS production may be involved in Smh-3-induced apoptotic cell death in HL-60 cells. The consistence of our data with our previous reports demonstrating that 2-phenyl-4-quinolone series compound induced apoptosis via ROS-dependent mitochondrial death pathway in human osteogenic sarcoma U-2 OS cells (22). When mitochondria receive an apoptotic signal, the outer membrane of mitochondria becomes permeabilized, and then cytochrome *c*, Apaf-1, procaspase-9, and AIF are released into the cytosol, activating caspase-3 and -7 by caspase-9, leading to apoptosis (23-25). Smh-3 induced the activation of caspase-9, -7 and -3 after 48 h treatment (Fig. 6), suggesting that Smh-3 may possibly activate intrinsic signaling pathways. Our results demonstrated an increase of ROS production after Smh-3 treatment for 3 h (Fig. 7), and then promoted the release of cytochrome *c*, Apaf-1 and AIF protein levels from mitochondria into the cytosol (Fig. 7). In addition, caspase-8 activity in Smh-3-treated HL-60 cells had no significant increase (Fig. 6). Based on the above evidence (Fig. 6), we might rule out that Smh-3-stimulated apoptotic cell death is involved in the extrinsic apoptotic pathway.

BCL-2 family proteins are classified into the following three categories according to their function: i) proteins were involved in inhibiting apoptosis: such as BCL-2, BCL-xL; ii) proteins were involved in promoting apoptosis: such as Bax, Bid; iii) BH3-only protein: such as BAD (23-25). BAD is activated by dephosphorylation, and has a conserved BH3 domain that binds and regulates the anti-apoptotic protein to promote cell apoptosis (10). Considerable evidence indicates that BAD can affect Bax by directly binding and inhibiting BCL-2 (26,27). Our study suggests that BAD was dephosphorylated and activated after HL-60 cells were treated with Smh-3 (Fig. 8C), which may lead to activation of Bax and inactivation BCL-2, then triggering apoptosis. It has been reported that AKT is involved in survival signaling pathway by phosphorylating BAD (11). The phospho-BAD bound to 14-3-3 proteins, but not BCL-2. In the present study, we demonstrated that Smh-3 inhibited the activity of AKT in HL-60 cells (Fig. 8A and B), leading to that BAD was reported to be deposphorylated and then induced apoptosis in Smh-3-treated HL-60 cells (11,28).

Overall, the molecular signaling pathways are summarized in Fig. 9. Our results demonstrated that Smh-3 exposure causes G_2/M phase arrest and inhibits AKT activity in HL-60 cells. Dephosphorylation of BAD promotes the releases cytochrome *c*, Apaf-1, AIF from mitochondria to cytosol which activates caspase-9, -7 and -3, leading to apoptosis. Hence, Smh-3 could possibly be used as a novel therapeutic agent for the treatment of leukemia in the future.

Acknowledgments

This study was supported by research grants from the National Science Council of the Republic of China awarded to S.-C. Kuo (NSC 98-2323-B-039-001) and L.-J. Huang (NSC 95-2320-B-039-011-MY3). Thanks are also due to support (in part) by the grant from the Department of Health (Taiwan), China Medical University Hospital Cancer Research Center of Excellence (DOH99-TD-C-111-005) and grant from China Medical University (CMU99-S-34).

References

1. Smith FO: Personalized medicine for AML? Blood 116: 2622-2623, 2010.
2. Nau KC and Lewis WD: Multiple myeloma: diagnosis and treatment. Am Fam Physician 78: 853-859, 2008.

3. Jegham H, Roy J, Maltais R, Desnoyers S and Poirier D: A novel aminosteroid of the 5alpha-androstane-3alpha,17beta-diol family induces cell cycle arrest and apoptosis in human promyelocytic leukemia HL-60 cells. Invest New Drugs (In press).
4. Suryadinata R, Sadowski M and Sarcevic B: Control of cell cycle progression by phosphorylation of cyclin-dependent kinase (CDK) substrates. Biosci Rep 30: 243-255, 2010.
5. Krystof V and Uldrijan S: Cyclin-dependent kinase inhibitors as anticancer drugs. Curr Drug Targets 11: 291-302, 2010.
6. Davis CD, Emenaker NJ and Milner JA: Cellular proliferation, apoptosis and angiogenesis: molecular targets for nutritional preemption of cancer. Semin Oncol 37: 243-257, 2010.
7. Caroppi P, Sinibaldi F, Fiorucci L and Santucci R: Apoptosis and human diseases: mitochondrion damage and lethal role of released cytochrome c as proapoptotic protein. Curr Med Chem 16: 4058-4065, 2009.
8. Burz C, Berindan-Neagoe I, Balacescu O and Irimie A: Apoptosis in cancer: key molecular signaling pathways and therapy targets. Acta Oncol 48: 811-821, 2009.
9. Russo AE, Torrisi E, Bevelacqua Y, *et al*: Melanoma: molecular pathogenesis and emerging target therapies (Review). Int J Oncol 34: 1481-1489, 2009.
10. Danial NN: BAD: undertaker by night, candyman by day. Oncogene 27 (Suppl. 1): S53-S70, 2008.
11. Kowalczyk JE and Zablocka B: Protein kinases in mitochondria. Postepy Biochem 54: 209-216, 2008.
12. Harvey RD and Lonial S: PI3 kinase/AKT pathway as a therapeutic target in multiple myeloma. Future Oncol 3: 639-647, 2007.
13. Yang JS, Hour MJ, Huang WW, Lin KL, Kuo SC and Chung JG: MJ-29 inhibits tubulin polymerization, induces mitotic arrest, and triggers apoptosis via cyclin-dependent kinase 1-mediated Bcl-2 phosphorylation in human leukemia U937 cells. J Pharmacol Exp Ther 334: 477-488, 2010.
14. Lu CC, Yang JS, Huang AC, *et al*: Chrysophanol induces necrosis through the production of ROS and alteration of ATP levels in J5 human liver cancer cells. Mol Nutr Food Res 54: 967-976, 2010.
15. Lo C, Lai TY, Yang JH, *et al*: Gallic acid induces apoptosis in A375.S2 human melanoma cells through caspase-dependent and -independent pathways. Int J Oncol 37: 377-385, 2010.
16. Lin SY, Lai WW, Ho CC, *et al*: Emodin induces apoptosis of human tongue squamous cancer SCC-4 cells through reactive oxygen species and mitochondria-dependent pathways. Anticancer Res 29: 327-335, 2009.
17. Ji BC, Hsu WH, Yang JS, *et al*: Gallic acid induces apoptosis via caspase-3 and mitochondrion-dependent pathways *in vitro* and suppresses lung xenograft tumor growth *in vivo*. J Agric Food Chem 57: 7596-7604, 2009.
18. Chou LC, Yang JS, Huang LJ, *et al*: The synthesized 2-(2-fluorophenyl)-6,7-methylenedioxyquinolin-4-one (CHM-1) promoted G2/M arrest through inhibition of CDK1 and induced apoptosis through the mitochondrial-dependent pathway in CT-26 murine colorectal adenocarcinoma cells. J Gastroenterol 44: 1055-1063, 2009.
19. Chen NG, Chen KT, Lu CC, *et al*: Allyl isothiocyanate triggers G2/M phase arrest and apoptosis in human brain malignant glioma GBM 8401 cells through a mitochondria-dependent pathway. Oncol Rep 24: 449-455, 2010.
20. Wang WJ: Acurhagin-C, an ECD disintegrin, inhibits integrin alphavbeta3-mediated human endothelial cell functions by inducing apoptosis via caspase-3 activation. Br J Pharmacol 160: 1338-1351, 2010.
21. Chen HY, Lu HF, Yang JS, *et al*: The novel quinolone CHM-1 induces DNA damage and inhibits DNA repair gene expressions in a human osterogenic sarcoma cell line. Anticancer Res 30: 4187-4192, 2010.
22. Hsu SC, Yang JS, Kuo CL, *et al*: Novel quinolone CHM-1 induces apoptosis and inhibits metastasis in a human osterogenic sarcoma cell line. J Orthop Res 27: 1637-1644, 2009.
23. Allan LA and Clarke PR: Apoptosis and autophagy: regulation of caspase-9 by phosphorylation. FEBS J 276: 6063-6073, 2009.
24. Gupta S: Molecular signaling in death receptor and mitochondrial pathways of apoptosis (Review). Int J Oncol 22: 15-20, 2003.
25. Decaudin D, Marzo I, Brenner C and Kroemer G: Mitochondria in chemotherapy-induced apoptosis: a prospective novel target of cancer therapy (Review). Int J Oncol 12: 141-152, 1998.
26. Levine B, Sinha S and Kroemer G: Bcl-2 family members: dual regulators of apoptosis and autophagy. Autophagy 4: 600-606, 2008.
27. Bergmann A: Survival signaling goes BAD. Dev Cell 3: 607-608, 2002.
28. Jiang P, Du W and Wu M: p53 and Bad: remote strangers become close friends. Cell Res 17: 283-285, 2007.